



## Unravelling the differential responses of critically endangered *Onobrychis conferta* populations to drought and salinity stress

A. SAKHRAOUI<sup>\*, \*\*, \*\*\*, +</sup>, H.B. LTAEIF<sup>\*\*</sup>, J.M. CASTILLO<sup>\*\*\*</sup>, and S. ROUZ<sup>\*\*</sup>

Higher School of Agriculture of Kef, University of Jendouba, 7119 Le Kef, Tunisia<sup>\*</sup>

Department of Agricultural Production – Laboratory of Agricultural Production Systems and Sustainable Development (SPADD), LR03AGR02, Higher School of Agriculture of Mograne, Carthage University, 1121 Mograne, Zaghouan, Tunisia<sup>\*\*</sup>

Department of Plant Biology and Ecology, University of Seville, Apartado 1095, 41080 Sevilla, Spain<sup>\*\*\*</sup>

### Abstract

Understanding stress responses of endangered plants is vital for their conservation under climate change. We examined the effects of iso-osmotic drought (PEG) and salinity (NaCl) on the growth and physiology of three populations of the critically endangered legume *Onobrychis conferta* subsp. *conferta* (OC1, OC2, OC3) endemic to North-Western Tunisia. Both stresses reduced photosynthesis, stomatal conductance, intercellular CO<sub>2</sub>, and carboxylation efficiency, while increasing intrinsic water-use efficiency. PSII photoinhibition (F<sub>v</sub>/F<sub>m</sub> decline) occurred after 6 d. Prolonged stress suppressed growth and water content, particularly under salinity, but enhanced root elongation and root-to-shoot ratios in OC1 and OC2. OC3, from dry grasslands, showed higher water retention, photosynthetic efficiency, and adaptive morphology than OC1 (*Pinus* forest) and OC2 (watercourse edge), highlighting ecotype-dependent tolerance. OC1 exhibited increased root allocation under salinity, exhibiting a salt-avoidance strategy. Identifying resilient ecotypes is crucial for conservation, restoration, and adaptation of *O. conferta* to increasing drought and salinity.

**Keywords:** chlorophyll; fluorescence; gas exchange; iso-osmotic stress; NaCl; sainfoin.

### Introduction

Abiotic stresses, such as drought and salinity, are major constraints to plant growth and survival, particularly in arid and semiarid regions (Munns and Tester 2008). They impair water relations, gas exchange, and photosynthesis, resulting in reduced biomass and fitness (Liu *et al.* 2025). With climate change predicted to intensify drought events

and soil salinization, understanding plant responses to osmotic and ionic stress is critical for identifying tolerant genotypes and ensuring the conservation of endangered species (Murtaza *et al.* 2025).

A recent meta-analysis indicates that climate change-driven drought and salinity have already altered plant morphology, physiology, and biochemistry, particularly in arid-region species (Dakhil *et al.* 2021). Ecosystems with

### Highlights

- *Onobrychis conferta* populations are more susceptible to ionic than osmotic stress
- Tolerance to polyethylene glycol and NaCl is ecotype-dependent
- Higher instantaneous carboxylation efficiency with lower net photosynthetic rate and stomatal conductance may support *O. conferta* stress tolerance

Received 27 August 2025

Accepted 11 November 2025

Published online 16 December 2025

<sup>+</sup>Corresponding author  
e-mail: anisak@alum.us.es

**Abbreviations:** C<sub>a</sub> – atmospheric CO<sub>2</sub> concentration; Chl – chlorophyll; C<sub>i</sub> – intracellular CO<sub>2</sub> concentration; F<sub>0</sub> – basal fluorescence; F<sub>m</sub> – maximum fluorescence; FM – fresh mass; F<sub>v</sub> – variable fluorescence; F<sub>v</sub>/F<sub>0</sub> – efficiency of the water-splitting complex; F<sub>v</sub>/F<sub>m</sub> – maximum photochemical efficiency of PSII; g<sub>s</sub> – stomatal conductance; IUCN – International Union for Conservation of Nature; L<sub>s</sub> – stomatal limitation; MDA – malondialdehyde content; PCA – Principal Components Analysis; PEG – polyethylene glycol; P<sub>N</sub> – net photosynthetic rate; TBA – thiobarbituric acid; TCA – trichloroacetic acid; WC – water content; WUE<sub>i</sub> – intrinsic water-use efficiency. **Acknowledgments:** The authors are very grateful to Prof. R. Rubio de Casas and Prof. F.J. Ocaña-Calahorro (Faculty of Sciences, University of Granada, Spain) for their valuable guidance and support. A. Sakhraoui sincerely thanks the University of Jendouba for granting a research fellowship.

**Conflict of interest:** The authors declare that they have no conflict of interest.

low floristic diversity appear more vulnerable to climate extremes, whereas biodiverse communities show greater functional resilience. Species with narrow ranges, notably Mediterranean endemics, are therefore at high risk, with models predicting severe range contractions under future scenarios (Dakhil *et al.* 2021). This highlights the urgency of conserving drought-resilient genotypes to sustain biodiversity and ecosystem functions (Wu *et al.* 2017a).

Drought and salinity driven by climate change are already altering plant morphological, physiological, and biochemical traits, especially in arid-region species (Dakhil *et al.* 2021). Low-diversity ecosystems are more vulnerable to climate extremes, while biodiverse communities show greater resilience. Narrow-ranged species, such as many Mediterranean endemics, face severe range contractions under future scenarios (Dakhil *et al.* 2021). Conserving drought-resilient genotypes is therefore critical to sustaining biodiversity and ecosystem functioning (Wu *et al.* 2017a). Ecosystems with low floristic diversity appear more vulnerable to climate extremes, whereas biodiverse communities show greater functional resilience (Dakhil *et al.* 2021). Similar findings have been reported for mangrove ecosystems in Guyana, where seedlings in degraded habitats showed altered growth and survival compared to those in restored or natural sites (Dookie *et al.* 2024).

The genus *Onobrychis* (sainfoin) includes forage legumes adapted to diverse and often harsh environments, with traits of interest for sustainable agriculture under climate change (Carbonero *et al.* 2011, Sakhraoui *et al.* 2023). While cultivated sainfoin (*Onobrychis viciifolia* Scop.) has been widely studied, little is known about wild relatives, such as *Onobrychis conferta* subsp. *conferta* (Desf.) Desv., particularly regarding their physiological responses to abiotic stress. This subspecies, native to arid and semiarid *Pinus halepensis* forests of North Africa (Pottier-Alapetite 1979), is distinguished by its silvery-silvery leaflets, hairy calyx teeth (Tison and de Foucault 2014), and pubescent pods with a radiating crest of triangular prickles (Pottier-Alapetite 1979). It is currently classified as Critically Endangered by the IUCN due to habitat fragmentation and anthropogenic pressures, including overgrazing (Sakhraoui *et al.* 2024a,b). Beyond its conservation value, *O. conferta* provides forage, fixes nitrogen, supports pollinators, hosts wildlife, and contributes to erosion control (Ríos *et al.* 1991). Recent work also shows that N<sub>2</sub>-fixing pioneer species play comparable roles in phosphorus cycling regardless of nodulation status, underscoring the broader biogeochemical importance of legumes in stressed ecosystems (Sun *et al.* 2025).

Several *Onobrychis* species occur in drought- and salt-prone habitats, including dry, calcareous, and saline soils in the Mediterranean, Irano-Turanian, and Central Asian regions, where water scarcity and high evapotranspiration act as strong selective pressures (Malisch *et al.* 2016, Wu *et al.* 2017a). *Onobrychis viciifolia* is widely cultivated in semi-arid steppes. Wild species such as *O. kabylica* and *O. caput-galli* thrive in rocky or salt-affected sites, reflecting notable adaptation to abiotic stress. Identifying

stress-tolerant *Onobrychis* populations is therefore vital for biodiversity conservation and for improving forage resilience and sustainability in degraded or marginal environments under climate change (Wu *et al.* 2017a).

The present study evaluated the responses of three *Onobrychis conferta* subsp. *conferta* populations from contrasting habitats to iso-osmotic drought and salt stress under controlled glasshouse conditions. We hypothesised that: (1) populations would be more susceptible to ionic than osmotic stress; (2) the population from dry grasslands would exhibit greater tolerance than that from watercourse edges; and (3) stress tolerance would be ecotype dependent, with isolated populations evolving distinct adaptive mechanisms.

## Materials and methods

**Study sites:** This study was conducted on three populations of *O. conferta* subsp. *conferta* from contrasted geographical regions and habitats. Pods were collected at the time of their natural dispersal in June 2019 from three populations (OC1, OC2, OC3) colonising grasslands and forest–grassland edges in distinct ecological zones in northwestern Tunisia within an upper semiarid bioclimate (Emberger 1976). Pods were randomly collected from at least 22 different mature plants per population to obtain an adequate representation of genetic diversity. The geographic locations of the collection sites were recorded using a GPS (*Garmin 72H receiver*, Olathe, Kansas, USA) (Fig. 1S, *supplement*). OC1 was found at 930 m elevation in Dyr El Kef (36°12'35.55"N, 8°44'32.90"E), under a *Pinus halepensis* plantation adjacent to cereal fields, with a temperate winter regime. The site receives 428.7 mm of rainfall annually and has a mean temperature of +18.5°C (Sakhraoui *et al.* 2024a). OC2 was located at 868 m in Ain Dyssa, Siliana (35°57'47.89"N, 9°15'22.16"E), on a steep slope within a *P. halepensis* forest at the edge of a seasonal watercourse, co-occurring with native species such as *Medicago tunetana* and *Hedysarum coronarium*, in a cool winter zone. It receives 384.6 mm of rainfall annually and has a mean temperature of +19.5°C. OC3 was sampled at 532 m in Kerib, Siliana (36°20'28.70"N, 9°7'50.53"E), from an overgrazed rocky grassland, an arid saline region, near an *Olea europaea* orchard, featuring species such as *Ampelodesmos mauritanicus* and the endemic *Onobrychis kabylica*. The site has a temperate winter climate, 454.8 mm of annual rainfall, and a mean annual temperature of +18.4°C (Sakhraoui *et al.* 2024a).

**Stress tolerance experiment:** Collected seeds of *O. conferta* subsp. *conferta* were cleaned, separated from the pods, and stored in paper bags at +15–25°C and 40–60% air relative humidity for 148 d until the beginning of the experiment. Our experiment was conducted in the glasshouse facility of the University of Granada (Spain) on 20 November 2019. The seed surface was sterilised with 5% hypochlorite for 15 s and thoroughly washed for 2 min with distilled water. In a previous germination test, we found that *O. conferta* seeds had a hard seed coat and

physical dormancy. Dormancy was broken by mechanical scarification, where seed coats were nicked with pliers until the endosperm of the seed became visible (Maldonado-Arciniegas *et al.* 2018). Then, seeds were placed on Petri dishes containing 10 mL of autoclaved medium solution containing 0.5% agar and 0.5% ammonium nitrate. Petri dishes were sealed with adhesive tape (*Parafilm*™) to prevent desiccation and placed in a germination chamber at  $+21 \pm 1^\circ\text{C}$  and 12/12 h (light/darkness) with a PPFD of 350  $\mu\text{mol m}^{-2} \text{s}^{-1}$ . Four days after germination, 60 morphologically uniform seedlings per population were transferred to multi-alveolar plates filled with vermiculite, upholstered with expanded clay and they were grown on distilled water for one week. One-week-old seedlings were transferred into vermiculite-filled plastic pots (300  $\text{cm}^3$ ; 7.8 cm diameter and 12.2 cm in height) watered with Hoagland solution (pH 6.5) (Hoagland and Arnon 1950) and grown under controlled glasshouse conditions at  $+20\text{--}25^\circ\text{C}$ , 50–60% humidity, and 16-h photoperiod with a PPFD of 350  $\mu\text{mol m}^{-2} \text{s}^{-1}$  at canopy level.

The experiment started when the plants were 90 d old and was designed in a completely randomised design with three populations, three treatments, and five replicates: Hoagland solution (control), 29% (w/v) polyethylene glycol (PEG) + Hoagland solution, and 300 mM NaCl + Hoagland solution. These two last treatments corresponded to an osmotic potential of  $-1.57 \text{ MPa}$  (Lan *et al.* 2020) to simulate the severe drought conditions occurring during summers in field conditions (Aïachi Mezghani *et al.* 2019). Just after ecophysiological nondestructive measurements, plants were collected 0, 3, 6, and 9 d after the beginning of the experiment ( $D_0$ ,  $D_3$ ,  $D_6$ , and  $D_9$ ) ( $n = 5$  plants per sampling day and treatment), and immediately frozen in liquid nitrogen and stored in a  $-80^\circ\text{C}$  freezer for further analyses.

**Biomass, water content, and morphological traits:** Shoot and root length, total number of leaves, total number of leaflets, shoot and root fresh mass, and shoot and root water content (WC) percentage were measured on  $D_0$ ,  $D_3$ ,  $D_6$ , and  $D_9$ . The total number of leaflets (NLf), number of leaves (NL), and the mean number of leaflets per leaf (NLf/NL, calculated as the ratio of NLf to NL) were recorded ( $n = 5$ ). Shoot (SL) and root length (RL) were measured manually using a ruler. Fresh mass (FM) was measured by weighing total leaf mass after harvesting. The dry mass (DM) was obtained after drying samples for over 72 h at  $+65^\circ\text{C}$ , and it was used to calculate the leaf water content, in percentage, for each plant:  $WC = [(FM - DM)/FM] \times 100$  (Martins *et al.* 2017).

**Leaf gas exchange:** Net photosynthetic rate [ $P_N$ ,  $\mu\text{mol}(\text{CO}_2) \text{ m}^{-2} \text{ s}^{-1}$ ], stomatal conductance [ $g_s$ ,  $\text{mol}(\text{H}_2\text{O}) \text{ m}^{-2} \text{ s}^{-1}$ ], and intracellular  $\text{CO}_2$  concentration [ $C_i$ ,  $\mu\text{mol}(\text{CO}_2) \text{ mol}^{-1}$ ] were measured just before harvesting using the *Li6800 Portable Photosynthesis System* infrared gas analyser (LICOR Inc., Lincoln, NE, USA). Intrinsic water-use efficiency (WUE) was calculated as  $P_N/g_s$  (Jaimez *et al.* 2005). Stomatal limitation ( $L_s$ ) was defined as  $1 - C_i/C_a$ , where  $C_a$  was the atmospheric  $\text{CO}_2$  concentration (Farquhar and Sharkey

1982). Measurements were performed on the youngest healthy and fully expanded leaves from the apical parts of the main stem of each plant ( $n = 5$  plants per treatment), in an open circuit under PPFD of 1,000  $\mu\text{mol m}^{-2} \text{ s}^{-1}$ ,  $+25.0^\circ\text{C}$ , and 400 ppm  $\text{CO}_2$  on sunny days ( $D_0$ ,  $D_3$ ,  $D_6$ , and  $D_9$ ) from 11:00 to 13:00 h (local time).

**Chlorophyll fluorescence:** Measurements of Chl *a* fluorescence were taken in the same leaves used for evaluation of gas exchange ( $n = 5$  plants per treatment) as described by Redondo-Gómez *et al.* (2010) using a *Handy PEA* fluorimeter (FMS-2, Hansatech Instruments Ltd., UK) on  $D_0$ ,  $D_3$ ,  $D_6$ , and  $D_9$ . Plants were dark-adapted for 20 min using leaf clips. Basal fluorescence in the dark-adapted state ( $F_0$ ) was measured using a modulated pulse [ $< 0.05 \mu\text{mol}(\text{photon}) \text{ m}^{-2} \text{ s}^{-1}$  for  $1.8 \mu\text{s}$ ] which was too small to induce significant physiological changes in the plant (Schreiber *et al.* 1986). Maximal fluorescence ( $F_m$ ) was measured after applying a saturating actinic pulse of  $18,000 \mu\text{mol}(\text{photon}) \text{ m}^{-2} \text{ s}^{-1}$  for 0.7 s. Values of variable fluorescence ( $F_v = F_m - F_0$ ) and maximum photochemical efficiency of PSII ( $F_v/F_m$ ) and the efficiency of the water-splitting complex ( $F_v/F_0$ ) were calculated (Maxwell and Johnson 2000).

**Photosynthetic pigments:** Adult and fresh leaf samples for photosynthetic pigments were collected during midday ( $n = 4$ ). Chlorophyll pigments were extracted in pure methanol. After centrifugation at  $+4^\circ\text{C}$ , the Chl *a*, Chl *b*, and total carotenoids (Car) content [ $\text{mg g}^{-1}(\text{DM})$ ] were determined spectrophotometrically at 470, 646, 652.4, and 665.2 nm by a *Hitachi U-2001* spectrophotometer (Hitachi Ltd., Tokyo, Japan). The contents were calculated according to Lichtenthaler and Buschmann (2001). The ratios Chl *(a+b)/Car* and Chl *a/b* were calculated.

**Free proline determination:** Foliar free proline determination was performed following the classical acid ninhydrin method as described by Carillo and Gibon (2011). Leaf material ( $n = 3$ ) was extracted in pure methanol, then 500  $\mu\text{L}$  of extract was mixed with 1 mL of reaction mix (acid ninhydrin 1% in acetic acid 60%, ethanol 20%), incubated for 1 h at  $+95^\circ\text{C}$  and cooled on ice. After, 1 mL of the mixture was used for reading the absorbance at 520 nm by a *Hitachi U-2001* spectrophotometer (Hitachi Ltd., Tokyo, Japan).

**Malondialdehyde determination** was assessed according to Taulavuori *et al.* (2001). Leaf material ( $n = 3$ ) was extracted in pure methanol, and 500  $\mu\text{L}$  of leaf extract was diluted with 100  $\mu\text{L}$  of pure methanol. Afterwards, 600  $\mu\text{L}$  of 20% trichloroacetic acid (TCA) reagent with 0.5% thiobarbituric acid (TBA) was added to the first tubes. Moreover, 600  $\mu\text{L}$  of 20% TCA reagent was added to the second tube. Subsequently, tubes were heated in a water bath at  $+95^\circ\text{C}$  for 15 min, after this time, the tubes were cooled on ice for 5 min. Samples were centrifuged at 12,000 rpm at  $+4^\circ\text{C}$  for 10 min. After, the supernatant was evaluated spectrophotometrically at 440, 532, and 600 nm by a *Hitachi U-2001* spectrophotometer (Hitachi Ltd., Tokyo, Japan).

**Data analysis:** All statistical analyses were performed using *IBM SPSS ver. 25* (SPSS Inc., Chicago, IL) for Windows, applying a significance level ( $\alpha$ ) of 0.05. Redundant, highly correlated variables ( $r > 0.95$ ) were identified before the analysis. Highly correlated variable ( $E$ ) was omitted from the statistical models. *Kolmogorov-Smirnov* test was performed to check for the validity of the normality assumption, and *Levene's* test for the homogeneity of variance. To meet the assumption of homogeneity of variances for parametric tests, Chl ( $a+b$ )/Car was transformed using  $\sqrt{x}$  function and Chl  $a/b$  using  $\ln(x)$ . The main univariate differences were evaluated for each functional plant trait using general linear models (LMs) with two grouping factors (population and treatment) and their interaction, and the *Bonferroni-Dunn* test as a *post-hoc* analysis. When homogeneity of variance was not achieved after data transformation, univariate differences were analysed using the  $\gamma$  generalised linear model (GLM) with *Wald's*  $\chi^2$ , differences were assessed using the *Kruskal-Wallis* nonparametric test (Ng and Cribbie 2017). Principal Components Analysis (PCA) was carried out, analysing the correlation matrix with 25 maximum iterations for convergence without rotation to extract independent PCA factors with eigenvalues  $> 1$ . The PCA was applied to the data matrix (39 morphological and physiological traits  $\times$  3 populations of *O. conferta*).

## Results

Population, stress treatments, and their interaction significantly affected growth and biomass, morphology, chlorophyll fluorescence, and photosynthetic responses (Table 1S, supplement).

**Biomass and morphological traits:** OC1 and OC2 populations showed decreased survival rates ( $-20$  and  $-40\%$ , respectively) under salt stress for 9 d (Fig. 1). The number of total leaflets and leaflets per leaf decreased

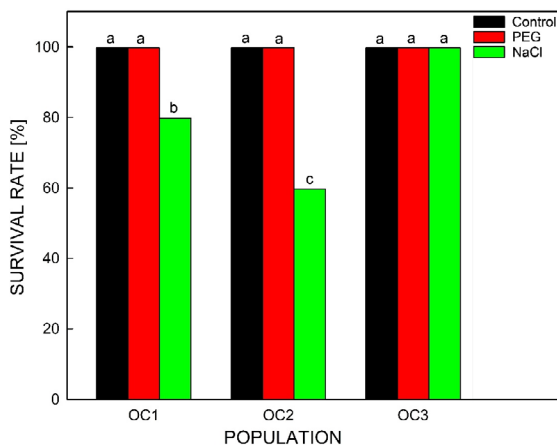


Fig. 1. Variations in survival rate of three different *Onobrychis conferta* populations under stressed and non-stressed conditions after 9 d. Values are mean  $\pm$  SE ( $n = 3$ ). Different letters above bar graphs indicate significant difference between populations (ANOVA,  $P < 0.05$ ).

after 9 d when subjected to salt stress for all studied populations. It remained unchanged when subjected to water stress (Fig. 2A,C). The decrease was especially pronounced for OC1 with  $ca.$   $-38$ ,  $-21$ , and  $-20\%$  reduction for the NLF, NL, and Nlf/NL after 9 d, respectively.

Imposing iso-osmotic drought and salt stress reduced shoot length significantly compared to the control (Fig. 2D). The reduction was the greatest ( $ca.$   $-13\%$ ) in OC2 plants after 9 d. Increased stress duration promoted root development by increasing the root length in the three populations. This increase was more prominent for OC2 after 9 d, reaching  $ca.$   $+34$  and  $+4\%$  under iso-osmotic and salt stress, respectively (Fig. 2E). The root-to-shoot length ratio was significantly higher in PEG than in NaCl-subjected plants, reaching  $ca.$   $+44$  and  $+20\%$  for OC2 and OC1 subjected to PEG and NaCl, respectively (Fig. 2F).

Depending on the decrease in shoot and root length, dry seedling mass decreased gradually with the increasing salt stress duration (Fig. 3). After 9 d of stress, the root dry mass decreased by  $ca.$   $-36$  and  $-17\%$  for OC2 and OC3, respectively (Fig. 3A,B). It increased by  $ca.$   $+43\%$  for OC1, compared to the control treatment. Shoot DM decreased in all the studied populations, especially in OC2 with  $ca.$   $-25\%$  under salt stress. The root-to-shoot DM ratio increased by  $ca.$   $+42.9\%$  for OC1 after 9 d under salt stress (Fig. 3C).

**Water content:** Significant differences were observed between populations, treatment and their interaction for shoot WC, while no significant difference in root WC between populations was recorded (Fig. 3). Both stresses decreased the shoot and root WC in the studied populations (Fig. 3D,E). A significant decrease in root WC of the three populations began after 6 d of stress. When compared to control, salt stress resulted in a higher decline of root and shoot WC after 9 d compared to iso-osmotic drought. Root water content decreased by approximately 21% and 15% under salt stress in OC1 and OC2, respectively, while shoot water content decreased by about 17% in OC1 and 21% in OC2.

**Leaf gas exchange:** Leaf gas-exchange traits were affected by population, stress treatments, and their interaction (Table 1S). The  $P_N$  and  $g_s$  of the three populations decreased progressively with stress time, reaching their lowest values at 9 d of treatment (Fig. 4). Overall, OC2 showed a significant decrease in  $P_N$ ,  $g_s$ , and  $C_i$  throughout the whole experiment. The highest decline in  $P_N$  was recorded for OC2, decreasing by  $ca.$   $-23$  and  $-81\%$  after 9 d under iso-osmotic drought and salt stress, respectively (Fig. 4A). Under salt stress,  $g_s$  declined significantly after 3 d in the three populations, reaching  $ca.$   $-80$  and  $-91\%$  for OC1 and OC2, respectively, when compared to control after 9 d (Fig. 4B). Under salt stress, an increase in  $C_i$  was observed after 3 and 6 d before decreasing significantly after 9 d for the three populations. Under drought,  $C_i$  decreased by  $ca.$   $-16$  and  $-28\%$  for OC1 and OC2, respectively (Fig. 4C). After 9 d of stress exposure, OC1 and OC2 had the highest  $WUE_i$  and  $L_s$  when

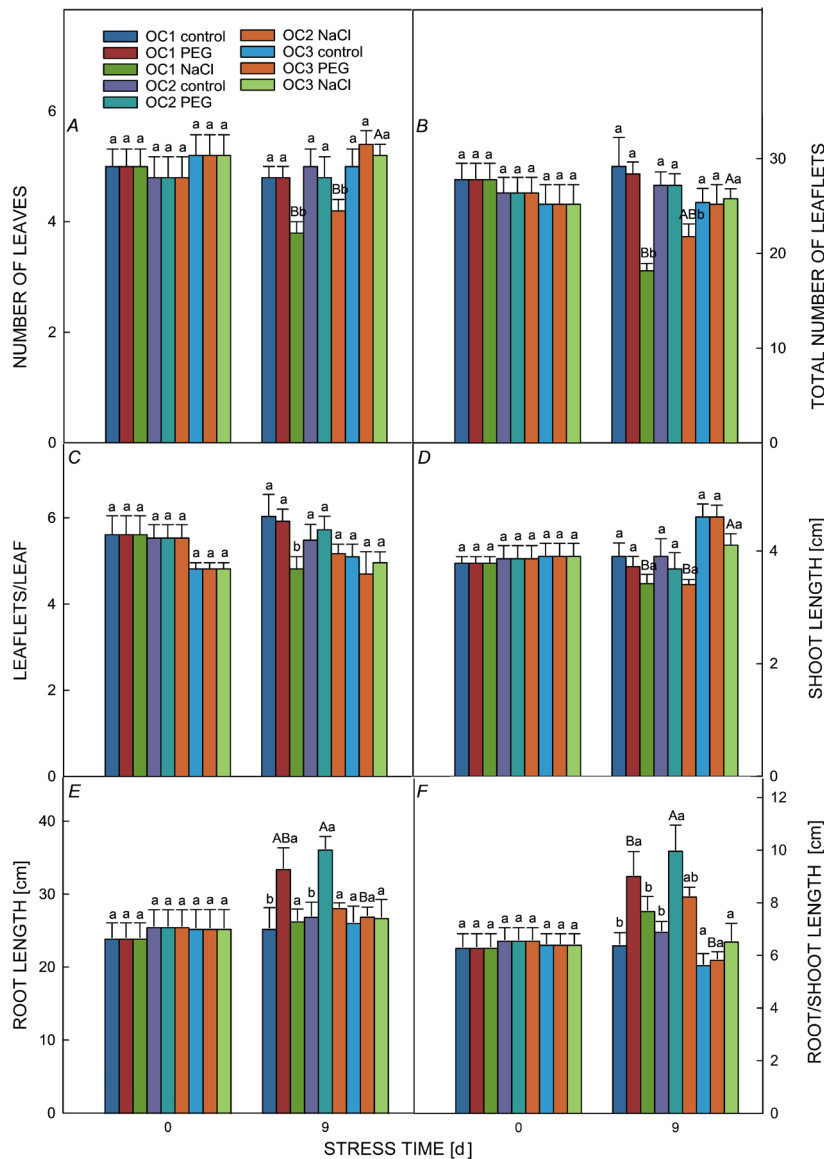


Fig. 2. Variations in (A) number of leaves, (B) number of leaflets, (C) number of leaflets per leaf, (D) shoot length, (E) root length, and (F) root/shoot length ratio of three different *Onobrychis conferta* populations under stressed and non-stressed conditions throughout the experimental timepoints. Values are mean  $\pm$  SE ( $n = 5$ ). Different letters indicate significant differences (Kruskal–Wallis test,  $P < 0.05$ ). Small and capital letters indicated a significant difference between treatments and populations, respectively.

compared with OC3. After 9 d of salt stress, WUE<sub>i</sub> was *ca.* +51 and +109% higher than control for OC1 and OC2 (Fig. 4D). For OC2, both stresses increased the WUE<sub>i</sub> and  $L_s$  significantly by *ca.* +26 and +93%, respectively, after 9 d (Fig. 4E). After 3 d of treatment, both stresses harmed the instantaneous carboxylation efficiency ( $P_N/C_i$ ) with maximum reduction recorded for OC2 under salt stress (*ca.* –74%) (Fig. 4F).

**Chlorophyll fluorescence:** Chl fluorescence traits were affected by population, stress treatments, and their interaction (Table 1S). The F<sub>m</sub> and F<sub>v</sub> declined significantly, while F<sub>0</sub> increased as both stresses progressed, especially after 9 d (Fig. 5A,C). Salt stress resulted in the highest decline in F<sub>v</sub> by *ca.* –60% for OC1 and OC2, respectively, compared to the control treatment. F<sub>m</sub> decreased by *ca.* –43 and –35% for OC1 and OC2, respectively. Under salt stress, F<sub>0</sub> increased by *ca.* +43 and +61% for OC3 and OC2, respectively. For OC1 and OC3, drought for 9 d did

not change F<sub>v</sub>/F<sub>m</sub> and F<sub>v</sub>/F<sub>0</sub>. However, only 3 d were enough to induce significant reductions in these efficiencies for OC2. Salt stress induced a significant decline in F<sub>v</sub>/F<sub>m</sub> and F<sub>v</sub>/F<sub>0</sub> after 3 d for the three populations (Fig. 5D,E).

**Photosynthetic pigments, MDA, and proline:** NaCl and PEG stress decreased the photosynthetic pigment contents (Chl *a*, Chl *b*, and Car) of *O. conferta* seedlings and increased the Chl (*a+b*)/Car ratio, and MDA and free proline contents (Fig. 6). After 9 d of treatment, Chl *a* and Chl *b* were *ca.* –71 and –67% lower in OC2, respectively, compared with the control. The maximum MDA and free proline content were observed after 9 d of treatment, increasing by *ca.* +163 and +152%, respectively, under salt stress for OC1 and OC2 (Fig. 6). After 9 d of stress, OC1 and OC3 had a +35 and +44% higher Chl (*a+b*)/Car, respectively, compared with the control.

**Principal component analysis:** The PCA biplot revealed distinct responses among the three *O. conferta* populations

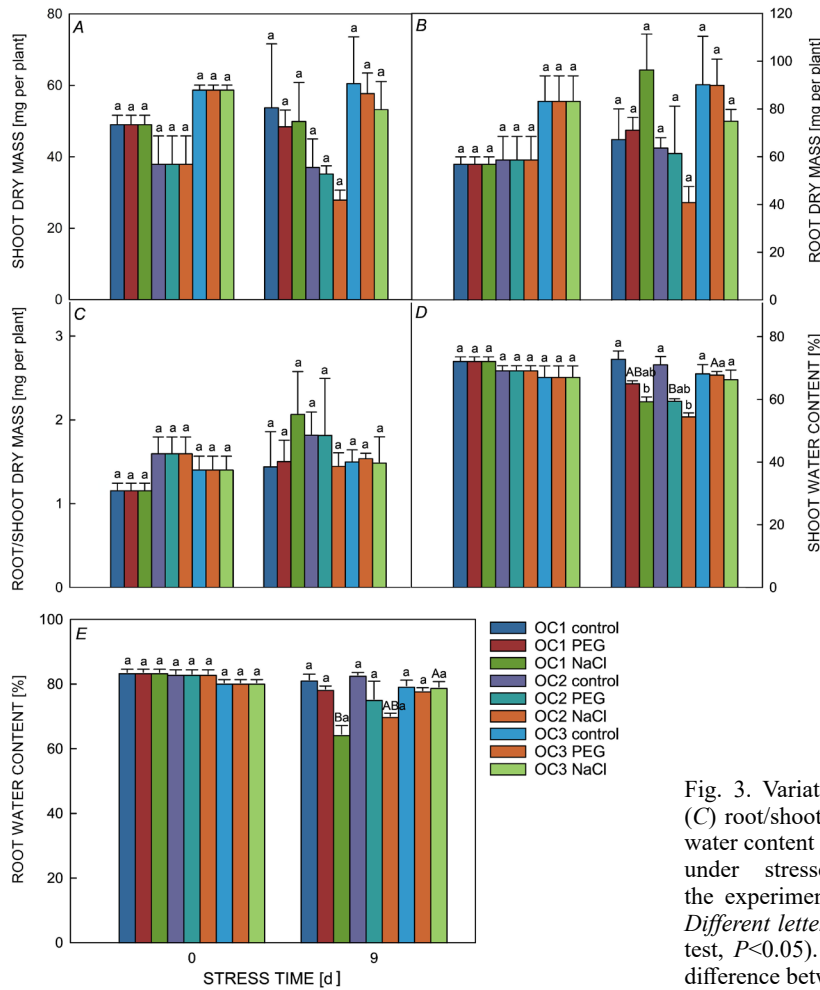


Fig. 3. Variations in (A) shoot dry mass, (B) root dry mass, (C) root/shoot dry mass, (D) shoot water content, and (E) root water content of three different *Onobrychis conferta* populations under stressed and non-stressed conditions throughout the experimental timepoints. Values are mean  $\pm$  SE ( $n = 3$ ). Different letters indicate significant differences (Kruskal–Wallis test,  $P < 0.05$ ). Small and capital letters indicated a significant difference between treatments and populations, respectively.

under osmotic stress and salt stress. Four components with an eigenvalue higher than 1 were detected in the PCA. Component 1, explaining 28.9% of the total variance and separating PEG-stressed samples from control and NaCl treatments, was mainly correlated with growth and shoot length, Chl content, and stomatal conductance. Stress-related markers, such as proline, malondialdehyde (MDA), and root/shoot ratios, were negatively correlated. The populations OC1 and OC3, under salt stress, were correlated with traits linked to better growth and physiological performance, indicating better tolerance. The population OC2 under salt stress showed a distinct separation along Component 2, explaining an additional 11.7% of the total variability, and was more closely related to MDA, suggesting a higher level of oxidative damage. PEG-treated samples, particularly from OC1, were associated with stress indicators, reflecting a strong osmotic stress response. Overall, OC3 exhibited the most balanced response to both treatments, while OC2 appeared more sensitive, especially under salt stress (Table 1; Fig. 2S, supplement).

## Discussion

Our results supported our hypothesis that iso-osmotic drought (from PEG) and salt (NaCl) stress negatively

affected survival, biomass, WC, Chl fluorescence, and gas exchange in all three *O. conferta* populations, with severity increasing over time. Populations were more sensitive to salt than to iso-osmotic drought. OC3, from an overgrazed rocky grassland, showed greater stress tolerance than OC1 and OC2, indicating better adaptation to harsh environments.

Osmotic stress alters root morphology, growth, and reproduction in *Onobrychis* under salinity and drought (Malisch *et al.* 2016, Wu *et al.* 2017a). Reduced root and shoot growth are typical plant responses to osmotic stress, largely because the stress limits root system expansion, which in turn restricts the plant's ability to explore the soil and absorb sufficient water and nutrients (Yuan *et al.* 2021). Salinity and drought lower root hydraulic conductivity, reducing water transport even in osmotically adjusted plants (Wu *et al.* 2017b). In our experiment, despite a general reduction in overall plant growth under prolonged salt and drought stress, root length increased in OC1 and OC2, likely because of enhanced meristematic activity in the root apex (Verslues and Longkumer 2022). The capacity of plants to withstand water deprivation depends not only on morphological adjustments but also on their ability to regulate the use of photoassimilates for water uptake, reflected in greater allocation of assimilates

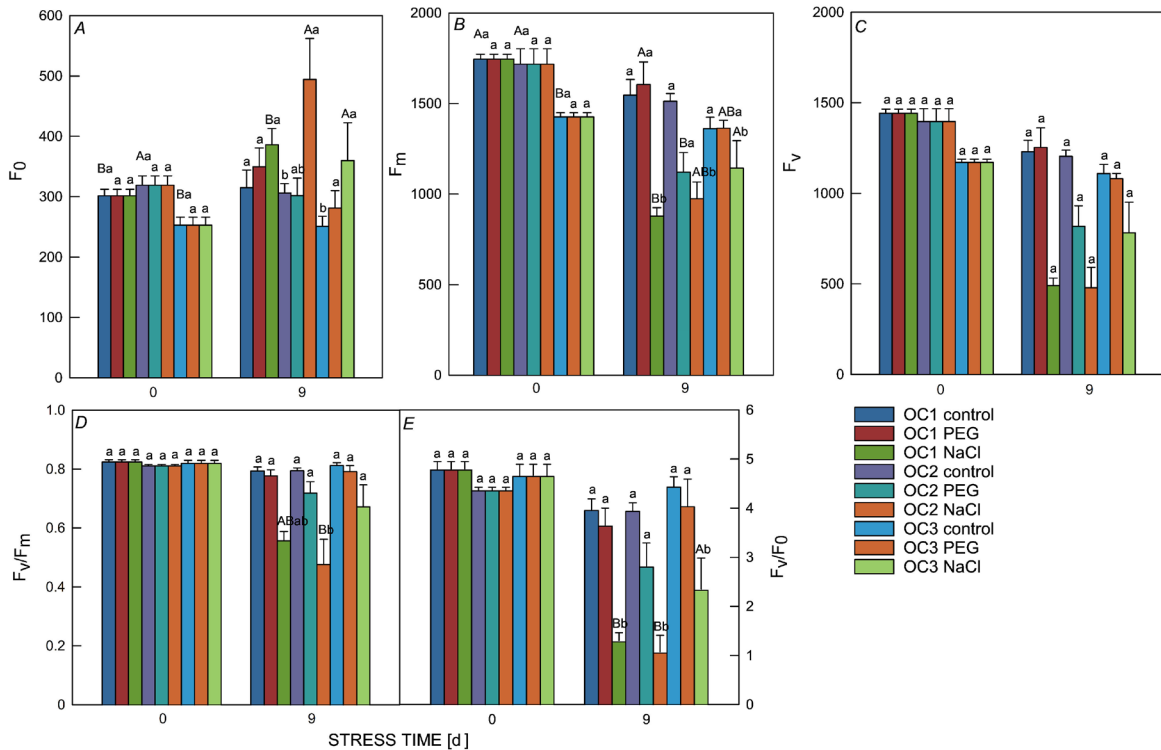


Fig. 4. Variations in (A) basal fluorescence ( $F_0$ ), (B) maximum fluorescence ( $F_m$ ), (C) variable fluorescence ( $F_v$ ), (D) maximum photochemical efficiency of PSII ( $F_v/F_m$ ), (E) efficiency of the water-splitting complex ( $F_v/F_0$ ) of leaves of three different *Onobrychis conferta* populations under stressed and non-stressed conditions throughout the experimental timepoints. Values are mean  $\pm$  SE ( $n = 5$ ). Different letters indicate significant differences (Kruskal–Wallis test,  $P < 0.05$ ). Small and capital letters indicated a significant difference between treatments and populations, respectively.

to the roots and, consequently, an increased root-to-shoot dry mass ratio (Yousefzadeh-Najafabadi and Ehsanzadeh 2021). This drought-induced root elongation may represent an adaptive response, allowing plants to access deeper soil layers where moisture and nutrients are more available. Such responses are often accompanied by increases in specific root length and the root-to-shoot dry mass ratio, indicating a preferential allocation of assimilates to root growth at the expense of shoots. These adjustments appear to be regulated by chemical signals during the early stages of drought and by hydraulic signals under prolonged stress, both of which reduce stomatal conductance and leaf expansion while sustaining root development (Yousefzadeh-Najafabadi and Ehsanzadeh 2021).

Such a strategy not only supports improved water and nutrient uptake but also contributes to ion dilution in plant tissues, thereby enhancing overall drought tolerance (Hussain *et al.* 2023). This investment in root traits is further beneficial because under stress conditions, root attributes, such as total root length and root density, become positively correlated with photosynthetic performance and stomatal conductance, suggesting that allocating a greater proportion of assimilates to roots helps maintain carbon assimilation and productivity under contrasting soil moisture conditions (Yousefzadeh-Najafabadi and Ehsanzadeh 2021).

Notably, the OC1 population responded to salt stress by allocating a greater proportion of biomass to root

development, primarily through enhanced root elongation. This response suggests a potential salt-avoidance strategy, where deeper root growth enables the plant to explore less saline soil layers and maintain water uptake under saline conditions (Munns and Tester 2008, Lynch 2013). Such an adaptive trait is considered beneficial for plant survival in salt-affected environments, as it allows partial escape from the ion-rich upper soil horizon (Tran *et al.* 2023). An increased root-to-shoot ratio confers several adaptive advantages under saline or drought-prone conditions. By reducing shoot biomass, plants lower their overall nutrient and water demands, particularly minimising transpiration losses through reduced leaf surface area (Munns and Gillham 2015). Concurrently, the preferential allocation of biomass to roots enhances soil resource acquisition, improving water and nutrient uptake efficiency from deeper or less saline zones – thereby contributing to improved stress tolerance and sustained growth under adverse conditions (Koevoets *et al.* 2016). Despite high salinity, genotypes that sustained higher root dry mass were better able to preserve total plant biomass, highlighting the role of root growth in buffering overall growth losses. In addition, the ability to maintain ionic homeostasis – particularly through  $K^+$  retention and  $Na^+$  exclusion – was linked to a smaller decline in root-to-shoot ratios, suggesting that biomass allocation to roots and ion balance act synergistically to enhance salt resilience (Abdehpour and Ehsanzadeh 2019).

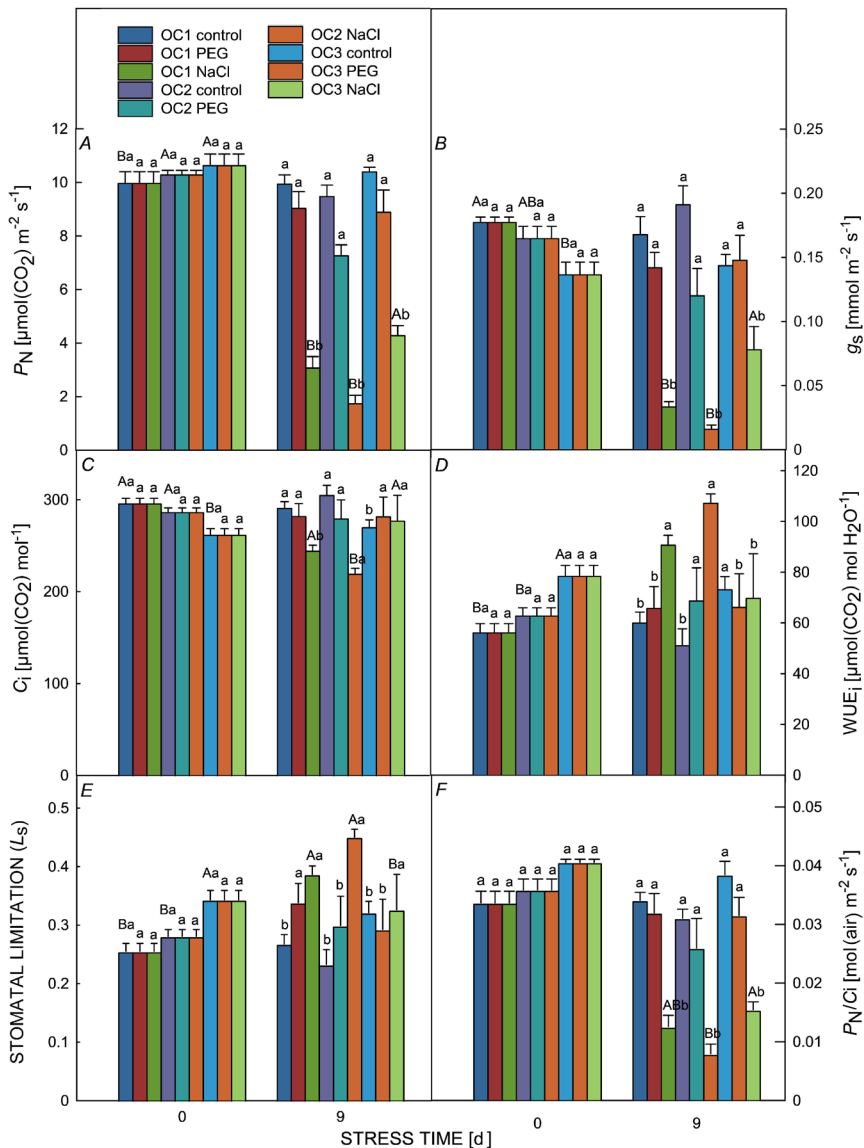


Fig. 5. Alterations in (A) net photosynthetic rate ( $P_N$ ), (B) stomatal conductance ( $g_s$ ), (C) intracellular  $\text{CO}_2$  concentration ( $C_i$ ), (D) water-use efficiency ( $\text{WUE}_i$ ), (E) stomatal limitation ( $L_s$ ), and (F) instantaneous carboxylation efficiency ( $P_N/C_i$ ) of three different *Onobrychis conferta* populations under stressed and non-stressed conditions throughout the experimental timepoints. Values are mean  $\pm$  SE ( $n = 5$ ). Different letters indicate significant differences (Kruskal–Wallis test,  $P < 0.05$ ). Small and capital letters indicated a significant difference between treatments and populations, respectively.

NaCl and PEG treatments significantly reduced shoot and root water content (WC) in the OC1 and OC2 populations, with salt stress causing the most pronounced decline in tissue hydration. This indicates stronger osmotic constraint under saline conditions, likely due to both ionic and osmotic components of salt stress (Munns and Tester 2008). In contrast, OC3 maintained higher shoot and root WC under PEG-induced drought stress than OC1 and OC2, suggesting an improved capacity to regulate internal water balance, potentially through more effective osmotic adjustment and cellular dehydration tolerance mechanisms (Yadav *et al.* 2022). The observed differences in WC between the three populations may reflect variation in xylem hydraulic conductivity, aquaporin activity, or root anatomical traits, which affect the efficiency of water transport under stress conditions. Such physiological traits are often shaped by natural selection in response to the contrasting moisture regimes and salinity levels of their ecogeographical origins (Sinclair *et al.* 2008, Sakhraoui *et al.* 2024a).

Drought and salinity stress reduced  $P_N$ , with variation observed between populations. The early PEG-induced decline in  $P_N$  appeared to be primarily associated with nonstomatal limitations, as  $g_s$  remained relatively constant (Ashraf and Harris 2013). After 9 d under drought and salinity, stomatal limitation became dominant (lower  $g_s$ ), which limits  $\text{CO}_2$  diffusion (Ma *et al.* 2025). Despite reduced  $P_N$ ,  $\text{WUE}_i$  increased due to greater reductions in  $g_s$ . The  $P_N/C_i$  ratio declined under stress, indicating reduced carboxylation efficiency and  $\text{CO}_2$  assimilation, with stomatal limitation playing a key role (Silva *et al.* 2015).

After 3 d of salt stress,  $F_0$  increased in all populations, indicating possible damage to the PSII core or reduced energy-trapping efficiency (Liu *et al.* 2019). This increase may also result from plastoquinone (PQ) accumulation and subsequent LHCII phosphorylation under stress (Krysiak *et al.* 2024). Elevated  $F_0$  is often linked to stress-related PSII inactivation or LHCII–PSII dissociation (Hu *et al.* 2023). Concurrently, a decrease in  $F_m$  suggests

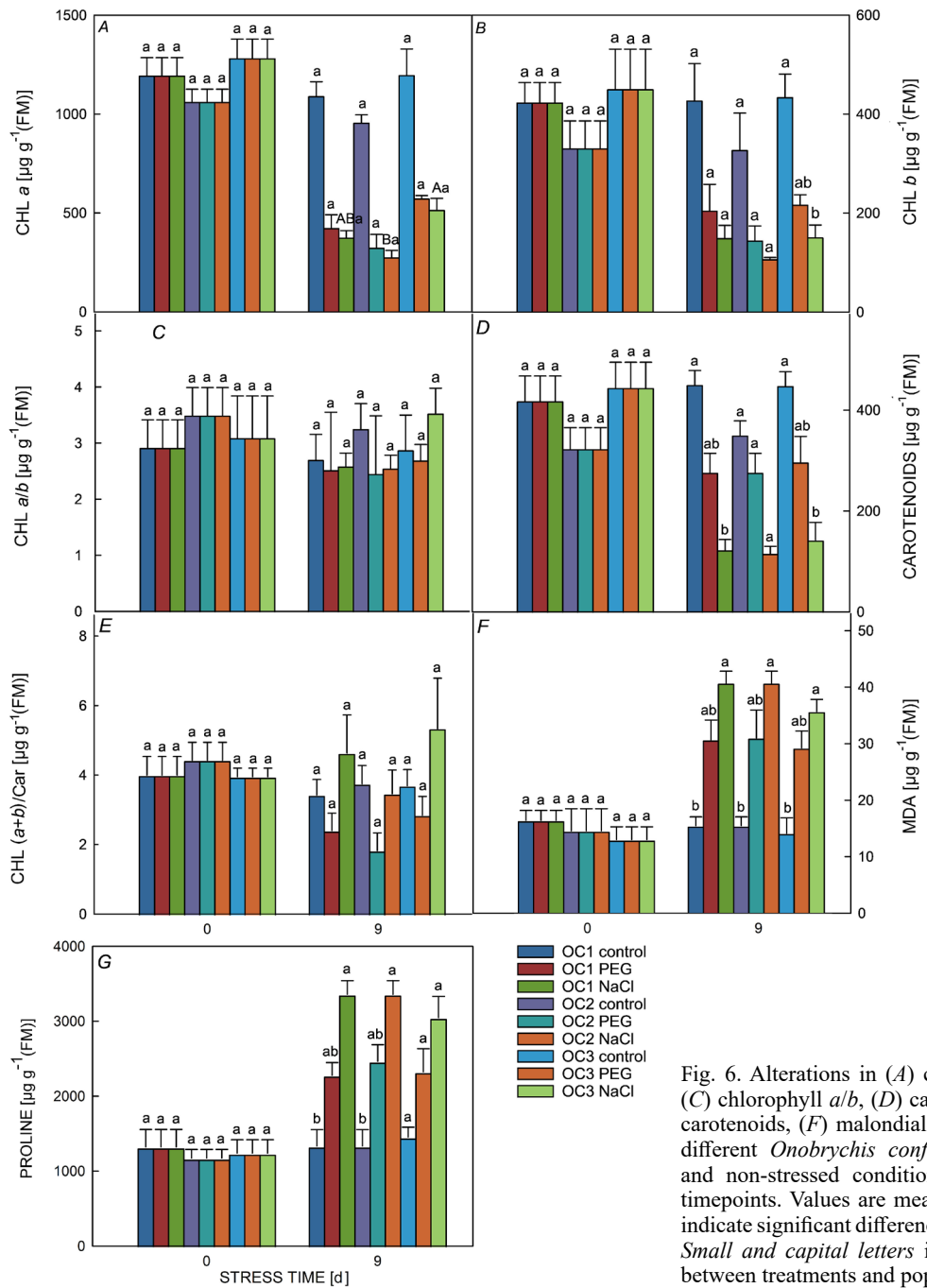


Fig. 6. Alterations in (A) chlorophyll *a*, (B) chlorophyll *b*, (C) chlorophyll *a/b*, (D) carotenoids, (E) chlorophyll (*a+b*)/carotenoids, (F) malondialdehyde, and (G) proline of three different *Onobrychis conferta* populations under stressed and non-stressed conditions throughout the experimental timepoints. Values are mean  $\pm$  SE ( $n = 3$ ). Different letters indicate significant differences (Kruskal–Wallis test,  $P < 0.05$ ). Small and capital letters indicated a significant difference between treatments and populations, respectively.

PSII inactivation and photoinhibition, possibly due to chloroplast damage or protein malfunction (Nawrocki *et al.* 2021, Bagchus *et al.* 2025). This decline reduces photochemical activity and  $\text{CO}_2$  assimilation (Dutra *et al.* 2017). Chl fluorescence, particularly  $F_v/F_m$  and  $F_v/F_0$ , declined significantly under drought and salt stress, signalling impaired PSII (Kalaji *et al.* 2018, Faseela *et al.* 2020). However,  $F_v/F_m$  alone may not reliably reflect photosynthetic performance (Dąbrowski *et al.* 2015), though it remains a useful indicator when combined with other fluorescence parameters and gas-exchange measurements (Dąbrowski *et al.* 2017, 2019). A drop in

$F_v/F_m$  under stress, in combination with decreased  $P_N$ , often reflects PSII damage and photoinhibition, highlighting its value for stress screening in crops (Wei *et al.* 2024). In the context of endangered species such as *O. conferta*, these physiological indicators are equally valuable for identifying stress-resilient populations, which is critical for targeted conservation actions. By assessing PSII efficiency and photosynthetic performance, conservationists can prioritise genetically robust populations for *in situ* protection, habitat restoration, or *ex situ* preservation efforts, thereby supporting the long-term survival of species under increasing environmental pressures.

Table 1. Factor loadings of plant trait obtained by Principal Component Analysis (PCA) for three *Onobrychis conferta* populations, three timepoints (0, 3, 6, and 9 d) and osmotic treatments (0, 29% w/v PEG and 300 mM NaCl). Correlations between the PCA and plant traits with factor loadings  $> \pm 0.600$  are marked in bold. Car – carotenoids content; Chl – chlorophyll;  $C_i$  – intracellular CO<sub>2</sub> concentration; F<sub>0</sub> – basal fluorescence; F<sub>m</sub> – maximum fluorescence; DM – dry mass; FM – fresh mass; F<sub>v</sub> – variable fluorescence; F<sub>v</sub>/F<sub>0</sub> – efficiency of the water-splitting complex; F<sub>v</sub>/F<sub>m</sub> – maximum photochemical efficiency of PSII; g<sub>s</sub> – stomatal conductance; L<sub>s</sub> – stomatal limitation; MDA – malondialdehyde content; P<sub>N</sub> – net photosynthetic rate; WC – water content; WUE<sub>i</sub> – intrinsic water-use efficiency.

	Component								
	1	2	3	4	5	6	7	8	9
Eigenvalues	9,252	3,729	2,996	2,737	2,083	1,877	1,624	1,297	1,209
Explained variance	28,913	11,654	9,362	8,553	6,508	5,866	5,075	4,055	3,780
Cumulative variance	28,913	40,567	49,928	58,482	64,990	70,856	75,931	79,985	83,765
Survival	0.192	-0.147	0.200	-0.066	-0.082	0.199	0.399	0.267	0.271
RL	-0.314	0.147	0.490	0.270	-0.012	0.591	-0.010	-0.141	-0.137
SL	0.145	0.112	0.060	0.538	-0.239	0.042	0.023	0.338	-0.421
SR ratio	0.416	0.052	0.467	-0.167	0.183	0.530	-0.015	-0.359	0.109
Leaflets	0.220	0.318	0.305	0.242	-0.264	0.182	0.665	0.078	-0.163
Leaves	0.088	0.052	0.306	0.529	-0.465	0.373	0.181	-0.257	-0.030
Leaflets/leaf	0.147	0.312	0.007	-0.319	0.277	-0.230	0.545	0.370	-0.179
Root FM	0.324	-0.187	0.030	<b>0.685</b>	0.480	-0.073	0.107	0.053	0.162
Shoot FM	0.424	<b>-0.676</b>	-0.416	0.261	0.099	0.103	0.220	-0.001	-0.054
Shoot/root FM	-0.139	<b>0.620</b>	0.424	0.331	0.289	-0.184	-0.150	0.057	0.210
Root DM	-0.209	-0.320	0.151	<b>0.689</b>	0.525	-0.088	-0.041	0.139	0.031
Shoot DM	0.190	<b>-0.735</b>	-0.377	0.268	0.268	0.254	0.132	0.010	-0.034
Shoot/root DM	-0.357	0.436	0.470	0.410	0.187	-0.330	-0.143	0.145	0.069
Root WC	<b>0.724</b>	0.189	-0.152	-0.094	-0.183	0.011	0.225	-0.070	0.130
Shoot WC	0.584	0.084	-0.063	0.173	-0.355	-0.333	0.211	0.013	-0.029
F <sub>0</sub>	-0.422	-0.333	0.023	-0.130	-0.075	0.378	-0.059	0.443	0.292
F <sub>m</sub>	<b>0.719</b>	0.046	0.181	-0.183	0.038	0.277	-0.055	0.313	0.391
F <sub>v</sub>	<b>0.813</b>	0.123	0.174	-0.151	0.055	0.187	-0.041	0.207	0.320
F <sub>v</sub> /F <sub>m</sub>	<b>0.835</b>	0.291	0.157	-0.075	0.077	-0.057	0.039	-0.070	0.034
F <sub>v</sub> /F <sub>0</sub>	<b>0.856</b>	0.303	0.044	-0.043	0.057	-0.065	0.005	-0.114	0.109
P <sub>N</sub>	<b>0.749</b>	0.400	-0.007	0.004	0.115	0.143	-0.172	0.046	-0.157
C <sub>i</sub>	0.298	<b>-0.628</b>	<b>0.632</b>	-0.140	-0.143	-0.234	-0.074	0.007	-0.070
g <sub>s</sub>	<b>0.782</b>	-0.061	0.349	-0.115	0.024	0.035	-0.197	0.062	-0.205
WUE <sub>i</sub>	-0.330	<b>0.617</b>	<b>-0.627</b>	0.143	0.137	0.229	0.082	-0.009	0.072
L <sub>s</sub>	-0.345	<b>0.619</b>	<b>-0.621</b>	0.118	0.132	0.235	0.051	-0.007	0.076
Chl a	<b>0.801</b>	-0.082	-0.196	0.242	-0.196	0.036	-0.230	-0.020	0.173
Chl b	<b>0.722</b>	-0.142	-0.029	0.061	0.217	-0.114	0.185	-0.350	0.158
Car	<b>0.802</b>	-0.098	-0.075	-0.064	0.251	0.219	-0.113	0.039	-0.206
Chl (a+b)/Car	-0.116	-0.063	-0.111	0.414	-0.500	-0.321	0.065	-0.194	0.459
Chl a/b	0.088	0.062	-0.242	0.289	-0.510	0.126	-0.456	0.386	-0.038
Proline	<b>-0.838</b>	-0.175	0.098	-0.027	-0.099	-0.067	0.157	0.081	0.120
MDA	<b>-0.813</b>	-0.122	0.159	-0.179	-0.003	-0.071	0.209	0.149	0.104

Free proline content was higher in OC1 and OC2 than in OC3, especially under salinity, denoting higher stress levels. This suggests that proline is a solute marker of drought and salinity that may alleviate oxidative damage (Wu *et al.* 2017a). Proline has been recognised as a multifunctional molecule, protecting cells from damage by acting as both an osmotic agent and a radical scavenger, and providing energy to drive growth once the stress is relieved (Kavi Kishor and Sreenivasulu 2014). In our study, PEG and especially NaCl induced significant drops in the Chl contents. The decrease in photosynthetic traits under salt stress could be explained by the effect of NaCl

that causes aggregation of adjacent grana membranes, shrinkage of thylakoids, and degradation of chlorophylls. It has been reported earlier that salinity decreases the P<sub>N</sub>, E, and g<sub>s</sub> and increases stomatal resistance (Ekinci *et al.* 2023).

As climate change intensifies the frequency and severity of drought and salinisation, especially in Mediterranean and North African regions (IPCC 2021), understanding intraspecific variation in stress tolerance becomes crucial for predicting population persistence and informing conservation strategies. Our findings have important implications for field performance, particularly

in the context of the varied ecogeographical origins of the three *O. conferta* populations. The differential stress responses observed under controlled conditions likely reflect adaptive divergence shaped by long-term exposure to contrasting environmental conditions. For instance, the superior stress tolerance of OC3, native to arid saline regions, underscores its potential as an ecotype pre-adapted to combined drought and salinity, making it a valuable genetic resource for restoration or breeding programs in dryland agriculture (Kooyers 2015, Prober *et al.* 2015). In contrast, the heightened sensitivity of OC1 and OC2 to ionic stress may reflect their origin from less saline habitats and suggests narrower ecological amplitudes. Our findings support the prioritisation of genetically diverse and stress-resilient populations in *ex situ* conservation efforts to safeguard the evolutionary potential of *O. conferta*, especially given its restricted distribution and threatened status (Sakhraoui *et al.* 2024a). This highlights the need to conserve genetically distinct ecotypes, particularly those showing stress tolerance, to preserve adaptive diversity and buffer against climate change impacts. Plant traits linked to stress tolerance, such as root elongation, improved water-use efficiency, and PSII stability, could inform the selection of genotypes for breeding or reintroduction efforts in degraded or arid regions. Ultimately, integrating ecophysiological traits with population origin data provides a powerful framework for both ecological restoration under future climates and the sustainable utilisation of native legumes in marginal environments.

## References

Abdehpour Z., Ehsanzadeh P.: Concurrence of ionic homeostasis alteration and dry mass sustainment in emmer wheats exposed to saline water: implications for tackling irrigation water salinity. – *Plant Soil* **440**: 427-441, 2019.

Aïachi Mezghani M., Mguidiche A., Allouche Khebour F. *et al.*: Water status and yield response to deficit irrigation and fertilization of three olive oil cultivars under the semi-arid conditions of Tunisia. – *Sustainability* **11**: 4812, 2019.

Ashraf M., Harris P.J.C.: Photosynthesis under stressful environments: an overview. – *Photosynthetica* **51**: 163-690, 2013.

Bagchus C., van Amerongen H., Wientjes E.: Photodamage and excitation energy quenching in PSII: A time-resolved fluorescence study in *Arabidopsis*. – *BBA-Bioenergetics* **1866**: 149569, 2025.

Carbonero C.H., Mueller-Harvey I., Brown T.A., Smith L.: Sainfoin (*Onobrychis viciifolia*): a beneficial forage legume. – *Plant Genet. Resour.* **9**: 70-85, 2011.

Carillo P., Gibon Y.: Protocol: extraction and determination of proline, 2011. Available at: <https://prometheusprotocols.net/function/tissue-chemistry/primary-metabolites/extraction-and-determination-of-proline/>.

Cornic G., Briantais J.-M.: Partitioning of photosynthetic flow between CO<sub>2</sub> and O<sub>2</sub> reduction in a C<sub>3</sub> leaf (*Phaseolus vulgaris* L.) at different CO<sub>2</sub> concentrations and during drought stress. – *Planta* **183**: 178-184, 1991.

Dąbrowski P., Baczevska-Dąbrowska A.H., Kalaji H.M. *et al.*: Exploration of chlorophyll *a* fluorescence and plant gas exchange parameters as indicators of drought tolerance in perennial ryegrass. – *Sensors* **19**: 2736, 2019.

Dąbrowski P., Kalaji M.H., Baczevska A.H. *et al.*: Delayed chlorophyll *a* fluorescence, MR 820, and gas exchange changes in perennial ryegrass under salt stress. – *J. Lumin.* **183**: 322-333, 2017.

Dąbrowski P., Pawłuskiewicz B., Baczevska A.H. *et al.*: Chlorophyll *a* fluorescence of perennial ryegrass (*Lolium perenne* L.) varieties under long term exposure to shade. – *Zemdirbyste* **102**: 305-312, 2015.

Dakhil M.A., Halmy M.W.A., Liao Z. *et al.*: Potential risks to endemic conifer montane forests under climate change: integrative approach for conservation prioritization in southwestern China. – *Landsc. Ecol.* **36**: 3137-3151, 2021.

Dookie S., Jaikishun S., Ansari A.A.: Comparative analysis of mangrove seedlings in natural, degraded, and restored ecosystems of Guyana. – *Geol. Ecol. Landsc.*, 1-18, 2024.

Dutra W.F., de Melo A.S., Dutra A.F. *et al.*: Photosynthetic efficiency, gas exchange and yield of castor bean intercropped with peanut in semiarid Brazil. – *Rev. Bras. Eng. Agríc. Ambient.* **21**: 106-110, 2017.

Ekinci M., Turan M., Ors S. *et al.*: Improving salt tolerance of bean (*Phaseolus vulgaris* L.) with hydrogen sulfide. – *Photosynthetica* **61**: 25-36, 2023.

Emberger L.: [Bioclimatic map of Tunisia according to Emberger's classification.] République Tunisienne, Institut National de Recherches Forestières, 1976. Available at: <https://esdac.jrc.ec.europa.eu/content/carte-bioclimatique-de-la-tunisie-selon-la-classification-demberger-ettes-et-variantes>. [In French]

Farquhar G.D., Sharkey T.D.: Stomatal conductance and photosynthesis. – *Annu. Rev. Plant Biol.* **33**: 317-345, 1982.

Faseela P., Sinisha A.K., Brestić M., Puthur J.T.: Chlorophyll *a* fluorescence parameters as indicators of a particular abiotic stress in rice. – *Photosynthetica* **58**: 293-300, 2020.

Hoagland D.R., Arnon D.I.: The Water-Culture Method for Growing Plants Without Soil. Pp. 32. California Agricultural Experiment Station, Berkeley 1950.

Hu C., Elias E., Nawrocki W.J., Croce R.: Drought affects both photosystems in *Arabidopsis thaliana*. – *New Phytol.* **240**: 663-678, 2023.

Hussain T., Asrar H., Zhang W., Liu X.: The combination of salt and drought benefits selective ion absorption and nutrient use efficiency of halophyte *Panicum antidotale*. – *Front. Plant Sci.* **14**: 1091292, 2023.

IPCC: Climate Change 2021: The Physical Science Basis. Contribution of Working Group I to the Sixth Assessment Report of the IPCC, 2021. Available at: <https://www.ipcc.ch/report/ar6/wg1/>.

Jaimez R.E., Rada F., García-Núñez C., Azócar A.: Seasonal variations in leaf gas exchange of platin cv. Hartón (*Musa AAB*) under different soil water conditions in a humid tropical region. – *Sci. Hortic.-Amsterdam* **104**: 79-89, 2005.

Kalaji H.M., Rastogi A., Živčák M. *et al.*: Prompt chlorophyll fluorescence as a tool for crop phenotyping: an example of barley landraces exposed to various abiotic stress factors. – *Photosynthetica* **56**: 953-961, 2018.

Kavi Kishor P.B., Sreenivasulu N.: Is proline accumulation *per se* correlated with stress tolerance or is proline homeostasis a more critical issue? – *Plant Cell Environ.* **37**: 300-311, 2014.

Koevoets I.T., Venema J.H., Elzenga J.T.M., Testerink C.: Roots withstanding their environment: exploiting root system architecture responses to abiotic stress to improve crop tolerance. – *Front. Plant Sci.* **7**: 1335, 2016.

Kooyers N.J.: The evolution of drought escape and avoidance in natural herbaceous populations. – *Plant Sci.* **234**: 155-162, 2015.

Krysiak M., Węgrzyn A., Kowalewska Ł. *et al.*: Light-independent pathway of STN7 kinase activation under low temperature stress in runner bean (*Phaseolus coccineus* L.). –

BMC Plant Biol. **24**: 513, 2024.

Lan C.-Y., Lin K.-H., Chen C.-L. *et al.*: Comparisons of chlorophyll fluorescence and physiological characteristics of wheat seedlings influenced by iso-osmotic stresses from polyethylene glycol and sodium chloride. – Agronomy **10**: 325, 2020.

Lichtenthaler H.K., Buschmann C.: Chlorophylls and carotenoids: measurement and characterization by UV-VIS spectroscopy. – Curr. Protoc. Food Anal. Chem. **1**: F4.3.1-F4.3.8., 2001.

Liu J., Lu Y., Hua W., Last R.L.: A new light on photosystem II maintenance in oxygenic photosynthesis. – Front. Plant Sci. **10**: 975, 2019.

Liu J., Wang Q., Zhan W. *et al.*: When and where soil dryness matters to ecosystem photosynthesis. – Nat. Plants **11**: 1390-1400, 2025.

Lynch J.P.: Steep, cheap and deep: an ideotype to optimize water and N acquisition by maize root systems. – Ann. Bot.-London **112**: 347-357, 2013.

Ma Y., Yuan Z., Wei Z. *et al.*: Stomatal and non-stomatal regulations of photosynthesis in response to salinity, and K and Ca fertilization in cotton (*Gossypium hirsutum* L.). – Environ. Exp. Bot. **230**: 106092, 2025.

Maldonado-Arciniegas F., Ruales C., Caviedes M. *et al.*: An evaluation of physical and mechanical scarification methods on seed germination of *Vachellia macracantha* (Humb. & Bonpl. ex Willd.) Seigler & Ebinger. – Acta Agron. **67**: 120-125, 2018.

Malisch C.S., Salminen J.-P., Kölliker R. *et al.*: Drought effects on proanthocyanidins in sainfoin (*Onobrychis viciifolia* Scop.) are dependent on the plant's ontogenetic stage. – J. Agr. Food Chem. **64**: 9307-9316, 2016.

Martins R.F.A., Souza A.F.C., Pitol C., Falqueto A.R.: Physiological responses to intense water deficit in two genotypes of crambe (*Crambe abyssinica* Hochst.). – Aust. J. Crop Sci. **11**: 821-827, 2017.

Maxwell K., Johnson G.N.: Chlorophyll fluorescence – a practical guide. – J. Exp. Bot. **51**: 659-668, 2000.

Munns R., Gillham M.: Salinity tolerance of crops – what is the cost? – New Phytol. **208**: 668-673, 2015.

Munns R., Tester M.: Mechanisms of salinity tolerance. – Annu. Rev. Plant Biol. **59**: 651-681, 2008.

Murtaza G., Ahmed Z., Iqbal R., Deng G.: Biochar from agricultural waste as a strategic resource for promotion of crop growth and nutrient cycling of soil under drought and salinity stress conditions: a comprehensive review with context of climate change. – J. Plant Nutr. **48**: 1832-1883, 2025.

Nawrocki W.J., Liu X., Raber B. *et al.*: Molecular origins of induction and loss of photoinhibition-related energy dissipation  $q_i$ . – Sci. Adv. **7**: eabj0055, 2021.

Ng V.K.Y., Cribbie R.A.: Using the gamma generalized linear model for modeling continuous, skewed and heteroscedastic outcomes in psychology. – Curr. Psychol. **36**: 225-235, 2017.

Pottier-Alapetite G.: [Flora of Tunisia: Angiosperms-Dicotyledons. Apetalous-Dialypetalous. Second part.] Pp. 406. Ministère de l'Enseignement Supérieur et de la Recherche Scientifique et le Ministère de l'Agriculture, Tunis 1979. [In French]

Prober S.M., Byrne M., McLean E.H. *et al.*: Climate-adjusted provenancing: a strategy for climate-resilient ecological restoration. – Front. Ecol. Evol. **3**: 65, 2015.

Redondo-Gómez S., Mateos-Naranjo E., Figueroa M.E., Davy A.J.: Salt stimulation of growth and photosynthesis in an extreme halophyte, *Arthrocnemum macrostachyum*. – Plant Biol. **12**: 79-87, 2010.

Ríos A., Correal E., Robledo A.: First screening of the more interesting pasture legumes present in matorral areas of south-east Spain. – In: Proceedings IV<sup>th</sup> International Rangeland Congress, Montpellier, France, 22–26 April 1991. Pp. 417-421. Association Française de Pastoralisme, Córdoba 1991.

Sakhraoui A., Ltacif H.B., Castillo J.M., Rouz S.: Habitat characterization and decline of critically endangered *Onobrychis conferta* subsp. *conferta*. – J. Nat. Conserv. **79**: 126603, 2024a.

Sakhraoui A., Ltacif H.B., Castillo J.M., Rouz S.: Genus *Onobrychis* (Fabaceae) in Tunisia: distribution, rediscovery, ecology, and description of two new variety with an updated identification key in the country – Phytotaxa **658**: 151-164, 2024b.

Sakhraoui A., Ltacif H.B., Sakhraoui A. *et al.*: Potential use of wild *Onobrychis* species for climate change mitigation and adaptation. – Crop Sci. **63**: 3153-3174, 2023.

Schreiber U., Schliwa U., Bilger W.: Continuous recording of photochemical and non-photochemical chlorophyll fluorescence quenching with a new type of modulation fluorometer. – Photosynth. Res. **10**: 51-62, 1986.

Silva F.G., Dutra W.F., Dutra A.F. *et al.*: [Gas exchange and chlorophyll fluorescence of eggplant grown under different irrigation depths.] – Rev. Bras. Eng. Agríc. Ambient. **19**: 946-952, 2015. [In Portuguese]

Sinclair T.R., Zwieniecki M.A., Holbrook N.M.: Low leaf hydraulic conductance associated with drought tolerance in soybean. – Physiol. Plantarum **132**: 446-451, 2008.

Sun S., Xie W., Wang G. *et al.*: Evidence for phosphorus cycling parity in nodulating and non-nodulating N<sub>2</sub>-fixing pioneer plant species in glacial primary succession. – Funct. Ecol. **39**: 985-1000, 2025.

Taulavuori E., Hellström E.-K., Taulavuori K., Laine K.: Comparison of two methods used to analyse lipid peroxidation from *Vaccinium myrtillus* (L.) during snow removal, reacclimation and cold acclimation. – J. Exp. Bot. **52**: 2375-2380, 2001.

Tison J.-M., de Foucault B.: [Flora Gallica: Flora of France.] Pp. 743. Biotope Éditions, Mèze 2014. [In French]

Tran K.-N., Pantha P., Wang G. *et al.*: Balancing growth amidst salt stress – lifestyle perspectives from the extremophyte model *Schrenkia parvula*. – Plant J. **116**: 921-941, 2023.

Verslues P.E., Longkumer T.: Size and activity of the root meristem: a key for drought resistance and a key model of drought-related signaling. – Physiol. Plantarum **174**: e13622, 2022.

Wei X., Han L., Xu N. *et al.*: Nitrate nitrogen enhances the efficiency of photoprotection in *Leymus chinensis* under drought stress. – Front. Plant Sci. **15**: 1348925, 2024.

Wu G., Liu H., Feng R. *et al.*: Silicon ameliorates the adverse effects of salt stress on sainfoin (*Onobrychis viciaefolia*) seedlings. – Plant Soil Environ. **63**: 545-551, 2017b.

Wu G.-Q., Feng R.-J., Li S.-J., Du Y.-Y.: Exogenous application of proline alleviates salt-induced toxicity in sainfoin seedlings. – J. Anim. Plant Sci. **27**: 246-251, 2017a.

Yadav M.R., Choudhary M., Singh J. *et al.*: Impacts, tolerance, adaptation, and mitigation of heat stress on wheat under changing climates. – Int. J. Mol. Sci. **23**: 2838, 2022.

Yousefzadeh-Najafabadi M., Ehsanzadeh P.: Correlative associations of photosynthetic and rooting attributes of sesame: Drought-induced reversed associations are corrected upon salicylic acid exposure. – S. Afr. J. Bot. **142**: 266-273, 2021.

Yuan T.-T., Xiang Z.-X., Li W. *et al.*: Osmotic stress represses root growth by modulating the transcriptional regulation of *PIN-FORMED3*. – New Phytol. **232**: 1661-1673, 2021.